

# Beam shaping assembly design of ${}^7\text{Li}(p,n){}^7\text{Be}$ neutron source for boron neutron capture therapy of deep-seated tumor

L. Zaidi<sup>a,\*</sup>, M. Belgaid<sup>a</sup>, S. Taskaev<sup>b,c</sup>, R. Khelifi<sup>d</sup>

<sup>a</sup> University of Science and Technology Houari Boumediene, Faculty of Physics, SNIRM Laboratory, BP 32 El Alia 16111, Bab Ezzouar 16111, Algeria

<sup>b</sup> Novosibirsk State University, st. Pirogova 2, Novosibirsk 630090, Russia

<sup>c</sup> Budker Institute of Nuclear Physics, Siberian Branch, Russian Academy of Sciences, pr. Akademika Lavrentieva 11, Novosibirsk 630090, Russia

<sup>d</sup> Saad Dahlab University, Departement of Physics, LPTHIRM Laboratory, BP 270 Soumaa, Algeria



## HIGHLIGHTS

- A neutron source from  ${}^7\text{Li}(p,n){}^7\text{Be}$  reaction based on a tandem accelerator vacuum insulation at Budker institute of nuclear physics is considered for Boron neutron capture therapy.
- The neutrons energies generated at 2.3 MeV proton energy are not suitable for treatment.
- A simple, cheaper and flexible beam shaping assembly for treatment of deep-seated tumors is proposed.
- The proposed BSA can fulfil the beam quality parameters recommended by IAEA.

## ARTICLE INFO

### Keywords:

Accelerator-based BNCT  
 ${}^7\text{Li}(p,n){}^7\text{Be}$  neutron generator reaction  
 Beam shaping assembly  
 In-phantom parameters

## ABSTRACT

The development of a medical facility for boron neutron capture therapy at Budker Institute of Nuclear Physics is under way. The neutron source is based on a tandem accelerator with vacuum insulation and lithium target. The proposed accelerator is conceived to deliver a proton beam around 10 mA at 2.3 MeV proton beam.

To deliver a therapeutic beam for treatment of deep-seated tumors a typical Beam Shaping Assembly (BSA) based on the source specifications has been explored. In this article, an optimized BSA based on the  ${}^7\text{Li}(p,n){}^7\text{Be}$  neutron production reaction is proposed.

To evaluate the performance of the designed beam in a phantom, the parameters and the dose profiles in tissues due to the irradiation have been considered.

In the simulations, we considered a proton energy of 2.3 MeV, a current of 10 mA, and boron concentrations in tumor, healthy tissues and skin of 52.5 ppm, 15 ppm and 22.5 ppm, respectively. It is found that, for a maximum punctual healthy tissue dose seated to 11 RBE-Gy, a mean dose of 56.5 RBE Gy with a minimum of 52.2 RBE Gy can be delivered to a tumor in 40 min, where the therapeutic ratio is estimated to 5.38.

All of these calculations were carried out using the Monte Carlo MCNP code.

## 1. Introduction

The concept of Boron Neutron Capture Therapy (BNCT) (Saurwein et al., 2012) is to provoke inside cancerous cells a nuclear reaction between accumulated boron-10 nuclei and thermal neutron for which the absorption cross section is extremely high. Thus, the cancerous cells can be destroyed by the resulting nuclei with high linear energy transfer (IAEA, 2001).

Two different neutron beams are commonly used for BNCT: the thermal neutron beam which limits the treatment to shallow tumors, such as skin melanoma, and the harder epithermal neutron beam

( $0.4\text{ eV} < E < 10\text{ keV}$ ) for deep-seated tumors (Zhou and Lee, 1997) such as glioblastoma multiform. The last one is the adequate in our case, since it is most effective deeper; it can penetrate deeper into tissues due to its high energy and can reach the thermal energy range after being slowed down by tissues. Epithermal beams thus allow patient treatment without surgical resection.

Various neutron sources are can be used for BNCT: reactor (Monshizadeh et al., 2015), accelerator based  ${}^9\text{Be}(p,xn)$  (Ceballos et al., 2011; Esposito et al., 2009), Linac uses photon target ( $e, \gamma$ ) and photo neutron source (Rahmani and Shahriari, 2011), D-T source (Eskandari and Kashian, 2009), accelerator based  ${}^7\text{Li}(p,n){}^7\text{Be}$ . The last has been

\* Corresponding author.

E-mail address: [liliazaidi16@gmail.com](mailto:liliazaidi16@gmail.com) (L. Zaidi).

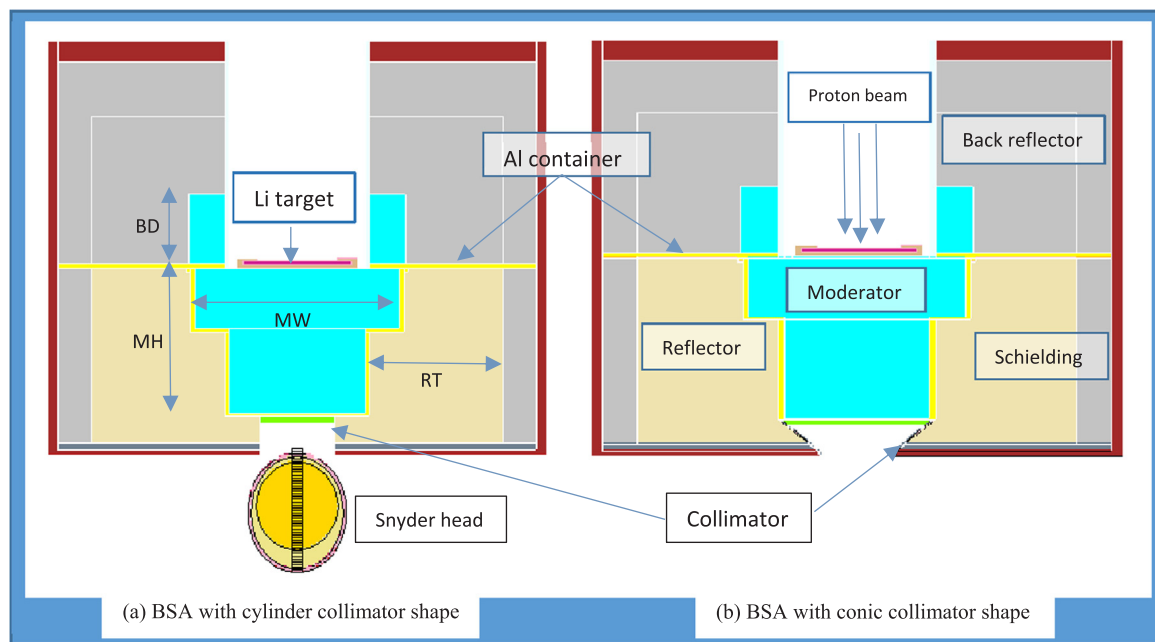


Fig. 1. Cross sectional view of the designed BSA configurations.

chosen due to the high neutron yield with relatively low energies at low energy of protons (Saurwein et al., 2012; Bayanov, 1998).

In this paper, the manufactured solid lithium target (Bayanov et al., 2004) and Vacuum Insulation Tandem Accelerator (VITA) (Taskaev, 2015) have been considered as a neutron source for BNCT. The energy of generated neutrons is higher than needed and should be moderated. In order to provide a therapeutic neutron beam, a special Beam Shaping Assembly (BSA) to optimize an epithermal neutron beam should be installed between the neutron source and the patient.

A typical BSA consists of a moderator to slow down fast neutrons to epithermal neutron energy ranges, a reflector to reduce neutron leakage out of the system, a collimator to focus neutrons to the patient position, gamma filter and thermal neutron filter (Monshizadeh et al., 2015).

Using MCNP code (X-5 Monte Carlo Team, 2003), different components of the BSA have been discussed and optimized. To evaluate the impact of the epithermal beam produced by the BSA in the human body the Snyder head phantom had been used, and in-phantom parameters had been calculated (Goorley et al., 2002).

The optimum configuration was chosen so that the tumors could be treated in the widest depth range at the shorter treatment time with the best therapeutic ratio.

## 2. Materials and methods

### 2.1. Neutron production (source)

The neutron generation is based on the reaction of protons on a metallic lithium target.

The neutron producing target assembly considered in the simulations consisted of a thin target lithium layer (100  $\mu\text{m}$ ) backing with micro channels of tantalum (0.4 mm thick) and convective water (2 mm thick), all of 10 cm diameter. Finally, copper of 3 mm thick for structural support.

The DROSG-2000 code (Drosg, 2005) was used to generate neutrons and calculate the yields. The double differential neutron yield per solid angle and energy were also calculated. The definition of the angular distribution was made for every 15 degrees to be introduced in MCNP code cards for source definition. The distributions were interpolated linearly between 13 defined points, from 0 to 180 degrees of the angle and energy distributions of the neutron yield.

The 478 keV inelastic scatter gammas and the radioactive capture ( $p,\gamma$ ) yields produced in the lithium target are reduced significantly by considering a thin target of lithium (Lee et al., 2000), and a backing material made of tantalum, where the remaining proton energy deposition will occur (Kasatov et al., 2015; Taskaev, 2015). Consequently, the gammas produced in the lithium target is too small at the beam port of the designed BSA, so it is neglected in all subsequent.

### 2.2. Beam shaping assembly

#### 2.2.1. Moderator

The emitted neutrons from the (Li,p) source belong to the fast energy range harder than those required for treatment, then cannot be used directly (Lee and Zhou, 1999). In order to reduce the energy of fast neutrons to the epithermal energy range, we explored different materials by a series of calculations.

The fact that the moderator should have a high scattering cross section at higher energies, lowest one for epithermal range and absorption cross section as small as possible, to avoid loss of neutron density and high radiative capture reaction, is to be taken into account. In addition, the closest distance from the exit beam side to the neutron source is a crucial parameter to increase neutron density (since the flux varies as  $1/r^2$ ); in this way, an optimized moderator can be obtained.

To reach the recommended values, many configurations were generated, the design processes of the moderator have been performed in two main phases:

- 1) Optimization of the moderator materials (with relatively low cost and high density),
- 2) Optimization of some geometry parameters such as the Moderator Width (MW), Moderator Height from the target to forward exit side of the BSA (MH), and target to Back Distance (BD), as shown in Fig. 1.

#### 2.2.2. Reflector

Neutrons generated from the target have an anisotropic distribution in direction and energy, moreover they used to be diffused in all directions after being scattered in the moderator and other components of the BSA like cooling water, structural support, etc.

To lead the neutrons in the desired direction, in our case forward, the reflector surrounds the moderator.

Knowing that the material with low absorption cross section and high elastic scattering cross section for epithermal neutron energies could be the appropriate one, we have investigated several materials, to cite some: Be, BeO, Al<sub>2</sub>O<sub>3</sub>, MgO in addition to the usual reflector materials, lead and graphite (Minsky and Kreiner, 2014; Culbertson et al., 2004).

We have calculated the thermal neutron flux ( $\Phi_{\text{ther}}$ ), epithermal neutron flux ( $\Phi_{\text{epi}}$ ), fast neutron flux ( $\Phi_{\text{fast}}$ ) and gamma flux ( $\Phi_{\gamma}$ ), using F2:N tally for neutrons and F2:P tally for photons in MCNP code. The calculations have been carried out for each material, and different thickness (RT) of the reflector surrounding the moderator and back-reflector, in order to choose the appropriate one.

### 2.2.3. Filters and collimator

To minimize the damage to healthy tissue nearby the tumor we need a higher convergence of the beam and a least possible contamination from fast neutrons, thermal neutrons and gamma ray.

The beam divergence variation is measured by  $J/\Phi$  factor (IAEA, 2001), which estimates the beam directionality. It is zero at the isotropic beam and one when it is parallel. The factor  $J/\Phi$  was calculated using F1 tally for neutrons current and F2 tally for neutrons flux through BSA aperture.

In order to increase beam convergence, a collimator has been added to the configuration, where the thickness, shape and composition were optimized.

In the last step, filters for thermal neutron absorption, moderation or scattering fast neutron and gamma rays shielding are explored.

Materials such Ti, Fe, <sup>32</sup>S have been tested for fast neutron contamination and Li-poly, LiF, Pb, Bi for shielding.

The gammas doses and the fast neutrons doses in-air were calculated using F4 tally MCNP cards and DE/Df cards for neutrons and gammas Kermas coefficients of tissue.

## 2.3. Dosimetry

Four principal physical dose components should be considered (IAEA, 2001):

- 1) Fast neutron dose ( $D_{\text{fn}}$ ) due to the proton recoil generated from <sup>1</sup>H (n,n)<sup>1</sup>H interaction.
- 2) Thermal neutron dose ( $D_{\text{N}}$ ) due to the energetic proton and the recoiling <sup>14</sup>C nucleus from the thermal neutron capture by <sup>14</sup>N via <sup>14</sup>N (n,p)<sup>14</sup>C reaction.
- 3) Boron dose ( $D_{\text{B}}$ ) from thermal neutron capture <sup>10</sup>B(n, $\alpha$ )<sup>7</sup>Li reaction.
- 4) Gamma dose ( $D_{\gamma}$ ) which is a combination of photon dose derived from the BSA and dose from photons induced by neutron capture reactions in tissues (Goorley et al., 2002).

The weighted total dose is defined as a sum of physical dose components multiplied by appropriate weighting-factors for each dose component in a tissue. It is denoted by  $D_{\text{w}}$ , and defined as follows (Palmer et al., 2002):

$$D_{\text{w}} = w_{\gamma}D_{\gamma} + w_{\text{B}}D_{\text{B}} + w_{\text{N}}D_{\text{N}} + w_{\text{fn}}D_{\text{fn}} \quad (1)$$

where  $D_{\text{w}}$  is the weighted total dose,  $D_{\gamma}$  is the gamma dose,  $D_{\text{B}}$  is the absorbed dose due to the boron,  $D_{\text{N}}$  is the nitrogen dose and  $D_{\text{fn}}$  is the fast neutron dose. The weighting factors  $w_{\text{N}}$  and  $w_{\text{fn}}$  were taken as 3.2,  $w_{\gamma}$  was considered to be 1.0 and  $w_{\text{B}}$  was considered 1.35, 3.8 and 2.5 in the normal tissue, tumor and skin, respectively (Busse et al., 2003).

To investigate the beam effect on patient body and beam performance, in-phantom parameters are calculated. These parameters are the ultimate measures for evaluating designed beam; we had estimated them by considering the treatment limitations such as maximum allowable dose for healthy tissue.

The in-phantom criteria are: Advantage Depth (AD), Advantage Ratio (AR), Treatable Depth (TD), AD Dose Rate (ADDR), and Treatment Time (TT) where:

AD is the depth in phantom at which the total therapeutic dose in tumor equals the maximum dose of the healthy tissue. AD indicates the depth of effective beam penetration (Sakamoto et al., 1999).

The AR is the ratio of the total therapeutic dose in tumor to the total normal tissue dose over a given depth (usually from the surface to AD). It is a measure of the therapeutic gain (Kiger et al., 1999).

TD is the depth at which the tumor dose falls below twice the maximum dose to normal tissue.

ADDR is defined as the maximum delivered dose to the healthy tissue.

As a representation of a patient head, an ellipsoidal head phantom based on the modified Snyder are considered. The elemental compositions for material of the analytical phantom: scalp, skull and brain taken from ICRU 46 (1992) of adult human head. The head was positioned at the exit side of the BSA (Fig. 1).

The <sup>10</sup>B concentrations in skin, brain and tumor were 22.5 ppm, 15 ppm and 52.5 ppm, respectively (Herera et al., 2013). Simulations were carried out to calculate thermal, epithermal and fast neutrons separately along the centre line of the beam through the brain. The four dose components using flux to dose conversion factors by means of MCNP F4 tally and DE4/DF4 cards, also investigated and a dose profiles in the head were got. Moreover, the parameters in phantom and the equivalent dose (for neutrons and photons) in each cell: skin, skull, brain and tumor tissue have been calculated, and the deposited energy distribution in the Snyder head phantom has been computed using a mesh tally option of MCNP code.

Statistical errors for the tallies were kept below 2% and the  $S(\alpha,\beta)$  thermal scattering treatment which takes into account the effects of chemical binding and crystal structure for reactions with incident neutron of thermal energy range, was used.

## 3. Results and discussion

### 3.1. Primary neutron

The primary neutron intensity at a beam target provided from the <sup>7</sup>Li(p,n)<sup>7</sup>Be reaction for different energy protons was evaluated using the DROSG-2000 code; the yields, double differential neutron yield per solid angle and energy were calculated. Increase of the proton energy leads to increase in neutron yield, but also the neutrons spectra become harder as it is shown in Fig. 2, where the neutron yield and maximum energy of the resulting neutrons depending proton beam energy are presented. Such calculations were previously performed in Lee and

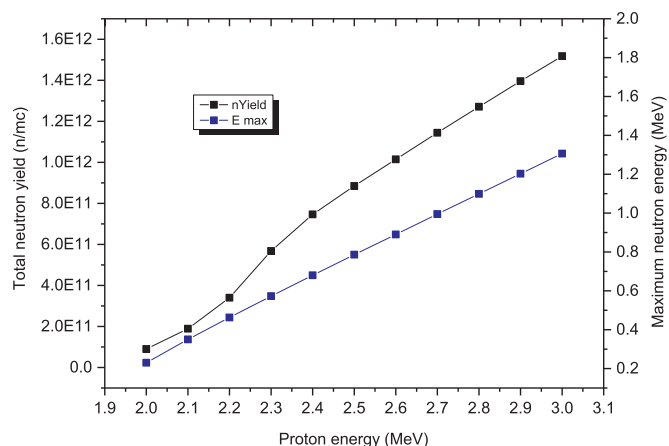


Fig. 2. Neutron yield and maximum energy of the resulting neutrons for <sup>7</sup>Li (p,n) reaction, depending proton energy.

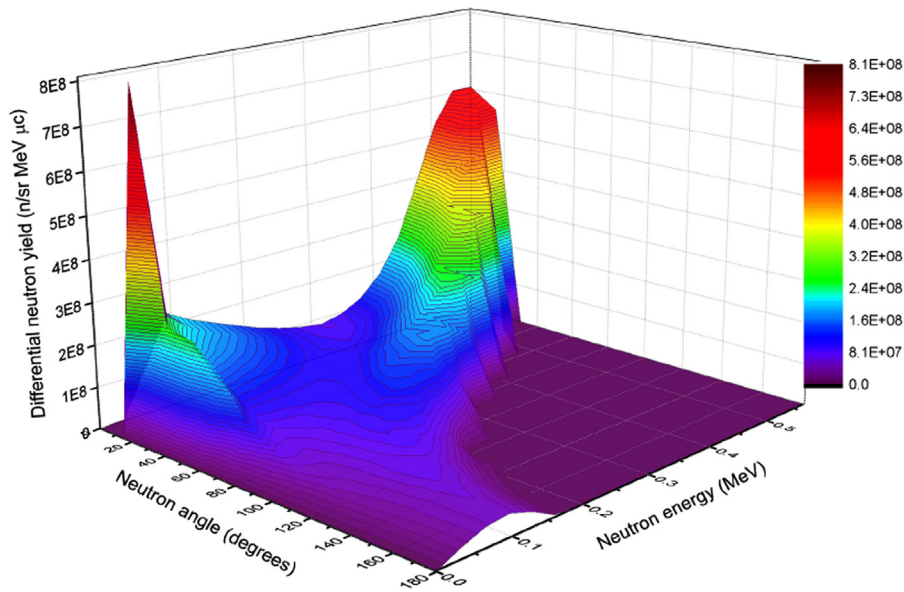


Fig. 3. Differential neutron yield for 2.3 MeV protons incident on thick lithium target.

Table 1  
Material's average logarithmic energy loss and density.

Material	MgF <sub>2</sub>	AlF <sub>3</sub>	BeO	Be	C	Pb	MgO
Density g cm <sup>-3</sup>	3.177	2.88	3.01	1.848	2.267	11.35	3.58
Av. log.E. loss (ξ)	0.098	0.098	0.175	0.230	0.158	0.018	0.101

Zhou (1999), Minsky and Kreiner (2014) and the results were the same.

We choose the value of the bombarding energy 2.3 MeV in order to take advantage of the resonance of <sup>7</sup>Li(p,n)<sup>7</sup>Be reaction at 2.25 MeV, and since the neutron intensity could be enough to generate a sufficient amount of epithermal neutrons for treatment 10<sup>9</sup> n/cm<sup>2</sup>; and not more than 2.3 MeV to decrease fast neutron flux.

The primary neutron yield generated by the <sup>7</sup>Li(p,n)<sup>7</sup>Be reaction assuming a beam energy of 2.3 MeV was estimated to be 576 n/pC, so for a current of 10 mA, 5.78 × 10<sup>12</sup> n/s can be reached for which the maximum energy is 573 keV and the mean energy is 233 keV. The double differential neutron yield per solid angle and energy is presented in Fig. 3.

The subsequent calculations of BSA optimization, neutron flux and dose estimation are based on the assumption of this primary neutron intensity at the target.

### 3.2. Beam shaping assembly results

#### 3.2.1. Moderator

Moderation of neutrons can be reached through collision with nuclei, thereby transferring some of their energy in the process. As a general rule, the light elements have the larger energy transfer per collision. However, the moderating material should have a considerable scattering cross section (σ<sub>s</sub>) at desirable neutron energies to be slowed down, and less absorption cross section (σ<sub>a</sub>). Light elements like hydrogen or beryllium containing moderator can reduce the neutron energy efficiently, but with an overly strong shift of the resulting neutron spectrum toward thermal energies, so that becomes inappropriate for the therapy of deeply seated tumors.

The σ<sub>s</sub> of some elements of interest with relatively low atomic mass were studied. We can notice important scattering cross sections at energies up to 25 keV in Al, F and Mg, and a significant neutron absorption at about 6 keV in Al, and a neglected σ<sub>a</sub> in the fluorine.

To take into account the energy loss through collisions, the average

logarithmic energy loss (ξ) defined as

$$\xi = \ln(A - 1/A + 1)^2 \tag{2}$$

is considered for the elements: Al, Mg, F, C, Be; their corresponding values (ξ) are 0.064, 0.081, 0.107, 0.158, 0.230. Moreover, since the moderation is proportional to the mean logarithmic energy and the macroscopic scattering cross section Σ<sub>s</sub>; where

$$\Sigma_s = n\sigma_s \tag{3}$$

the density (n) of the composite elements: MgF<sub>2</sub>, AlF<sub>3</sub>, BeO, Be and C reported in Table 1 and their absorption cross section (σ<sub>a</sub>), are considered to choose the good moderator.

Using a moderator containing fluoride is a good choice to moderate fast neutrons generated from <sup>7</sup>Li(p,n)<sup>7</sup>Be reaction with 2.3 MeV proton energy to epithermal range (Zaidi et al., 2017), thus, in this work MgF<sub>2</sub> was used as a moderator.

#### 3.2.2. Reflector

As the next step Be, BeO, Al<sub>2</sub>O<sub>3</sub>, MgO, C and Pb forward reflector materials have been tested. The variation of the neutron flux corresponding to different thickness of the reflector for each element calculated at the exit port are presented in Fig. 4, where (a) shows the total neutron flux variation, (b) epithermal neutron flux, (c) fast neutron flux, and (d) thermal flux.

The useful flux increases with increasing reflector thickness, for thickness up to 25 cm the epithermal flux increases slightly to its asymptotic value by 4–2% for almost reflectors, while increasing of reflector thickness beyond 20 cm generates more thermal neutrons in the reflector. This increases the gamma-ray from the neutron capture reactions, without increasing significantly the epithermal neutron.

To choose the best material for the reflector, we also analyzed the epithermal to thermal neutron ratio, and epithermal to fast neutron ratio shown in Fig. 5 and Fig. 6, respectively.

We can see that we have a highest epithermal to thermal ratio in case of Al<sub>2</sub>O<sub>3</sub> and Pb reflector, but lower for epithermal to fast neutron ratio. Using Al<sub>2</sub>O<sub>3</sub> is not interesting because it shows less epithermal neutron amount comparing to the others, otherwise in using Pb the moderator height should be increased, which causes also the flux decrease.

In terms of epithermal neutron for 20 cm thickness BeO, Be, C and MgO are close, they have the highest amounts of epithermal neutrons, see Fig. 4(c). Besides, MgO represents less contamination of thermal

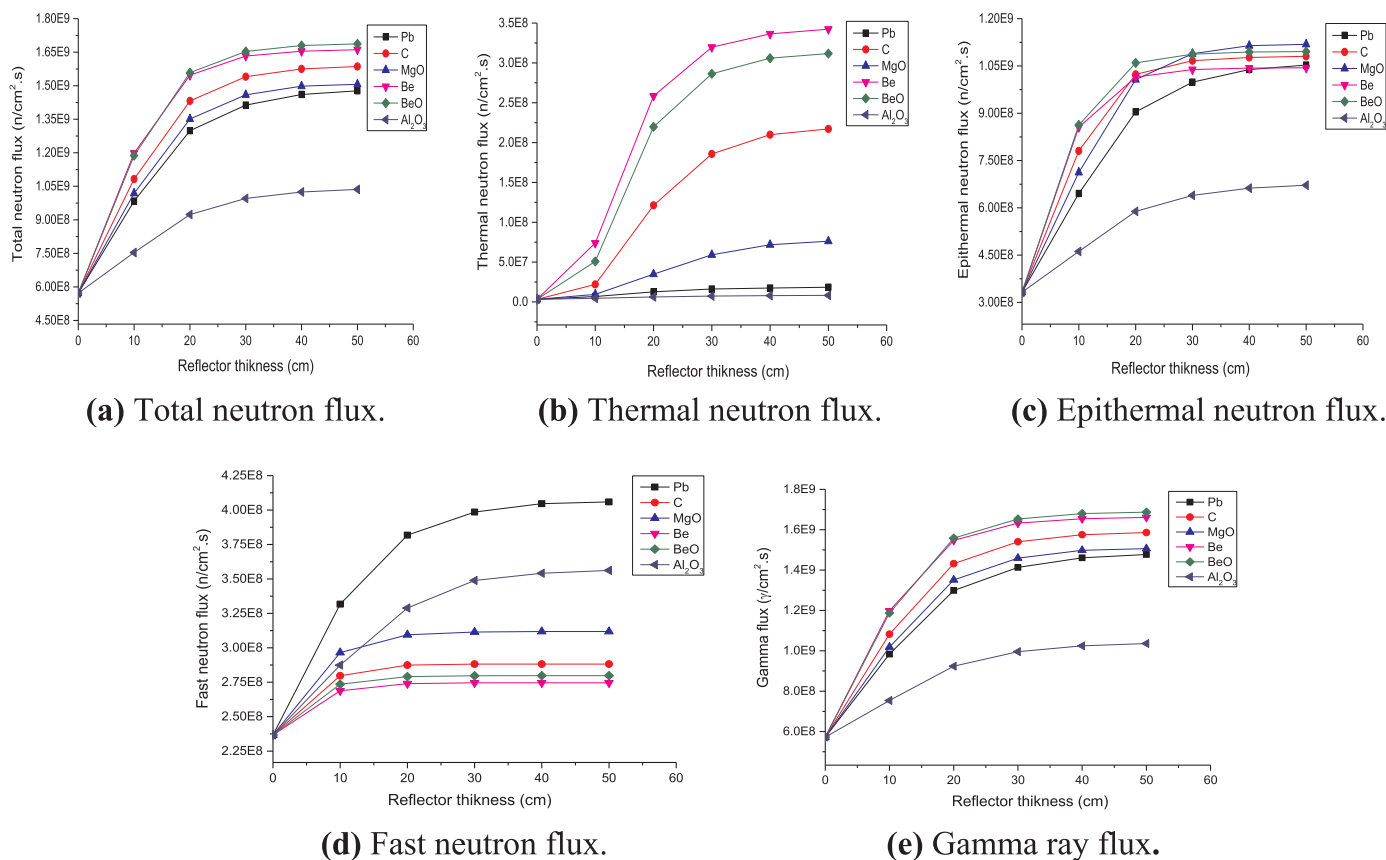


Fig. 4. Fluxes depending sizes of the reflectors.

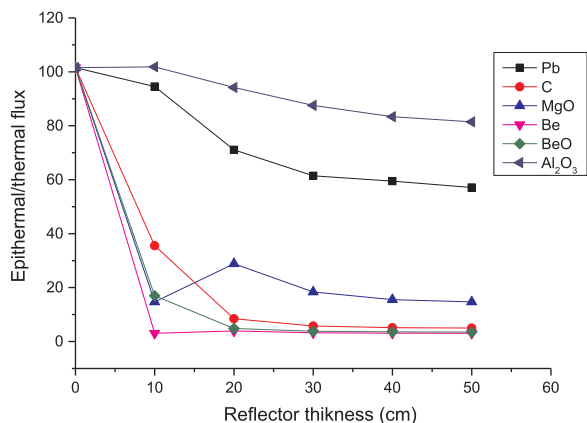


Fig. 5. Epithermal to thermal neutron flux ratio.

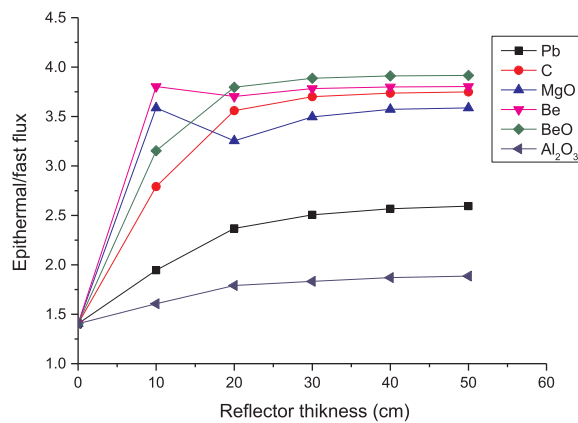


Fig. 6. Epithermal to fast neutron flux ratio.

neutrons comparing to BeO, Be and C, see Fig. 4(b). In addition, less gamma flux contamination after Al<sub>2</sub>O<sub>3</sub> and Pb.

Thus, the appropriate reflector for our configuration is 20 cm MgO. In this case we need not thick filters for thermal neutrons and gamma ray, conducting to decrease the epithermal one, comparing to use of BeO, Be or C. Also, no need to increase the moderator to slow down fast neutrons, which is recommended in case of Pb.

Magnesium oxide has an adequate property in terms of scattering of epithermal neutrons, and slowing down the fast neutrons not too much; owing to a relatively large mass number, in which not a lot of energy is lost with elastic collisions ( $\xi = 0.09$ ), contrary to Be or C for which  $\xi$  is 0.218 and 0.145, respectively.

In the back reflector it found suitable to use a part of moderator (Minsky and Kreiner, 2014). In our case we tested MgF and MgO surrounding the target and compared to the use of only Pb, or only C, and

it was found that 10 cm MgF<sub>3</sub> in the back allowed to get more epithermal neutrons, whereas Pb alone reflects more fast neutrons, and C more thermal neutrons.

### 3.2.3. Collimator and filters

To converge the neutrons to a local radiation, which leads to decrease of dose delivery to healthy tissue, after the moderator we contracted the BSA beam port to a flat circular surface of 10 cm diameter surrounded by the reflector.

To avoid undesirable thermal neutrons and gamma rays contamination in the beam, a 1 mm Bi layer, and 1 mm enriched lithiated-polyethylene with <sup>6</sup>Li were chosen to cover the collimator. This thickness was desired so that not to decrease significantly the epithermal flux and to be still not harmful with some contaminations.

The flux decreased by 48.3% and 6.8% for the thermal neutrons and

**Table 2**  
Comparison of beam quality parameters between different neutron beams designed and the IAEA recommended values.

Parameters	$\Phi_{\text{epi}}$ (n/cm <sup>2</sup> s)	$\Phi_{\text{epi}}/\Phi_{\text{ther}}$	$D_{\text{fn}}/\Phi_{\text{epi}}$ (Gy $\cdot$ cm <sup>2</sup> )	$D_{\gamma}/\Phi_{\text{epi}}$ (Gy $\cdot$ cm <sup>2</sup> )	$J/\Phi$
IAEA recommendation	$> 10^9$	$> 20$	$< 2 \times 10^{-13}$	$< 2 \times 10^{-13}$	$> 0.7$
Cylinder collimator	1.04E+ 09	2.94E+ 01	1.25E-13	1.89E-13	6.57E-01
Conic collimator	1.17E+ 09	2.83E+ 01	1.46E- 13	2.50E- 13	6.52E- 01
Cylinder without Ti	1.09E+ 09	2.56E+ 01	1.93E- 13	1.49E- 13	6.62E- 01
Conic without Ti	1.26E+ 09	2.41E+ 01	2.19E- 13	1.28E- 13	6.54E- 01
12 cm conic collimator without Ti	1.02E+ 09	2.95E+ 01	1.67E- 13	1.07E- 13	6.67E- 01

epithermal ones, respectively, at using 1 mm of lithiated-polyethylene and 1 mm Bi. While it decreased by 96.8% and 23.4% when LiF was used. Fig. 8 shows the flux variation for different thickness of the filters.

After dose calculations it is found that it is better to use Li-poly, where the delivered dose is greater and the therapeutic ratio is higher.

In addition of materials composing the beam port, a conic-shape of collimator and a simple cylinder with different dimensions were tested, in Table 2 the free beam parameters are presented.

In our case we found that for 5.8 cm of collimator's size it is enough and it is better to use a cylindrical shape, because we have less fast neutrons and thermal neutrons contamination. Moreover, the ratio  $J/\Phi$  is a little bit smaller in case of the conic collimator. Current to flux ratio  $J/f$  of the BSA is increased from 0.617 to 0.657 adding the collimator. The radial distribution at beam port for a BSA with and without a cylinder shape collimator is presented for neutrons and gamma-rays in Fig. 7.

The final BSA is shown in Fig. 9, it consists of MgF<sub>2</sub> moderator surrounded by MgO reflector. An external layer of poly-lithium and lead shields from thermal neutrons and gamma rays, respectively. The 10 cm diameter port has a 1 cm Ti, 1 mm Bi layer and 1 mm lithiated-polyethylene to avoid undesirable fast neutrons, thermal neutrons and gamma rays contamination in the beam.

Fig. 10 shows neutron energy spectrum corresponding to the optimal BSA with energies centered on 10 keV, which is considered to be the ideal spectrum for treating deep-seated tumors. The beam generated consists of 85.1% epithermal neutron flux, where the undesirable fast neutron dose per epithermal neutron is 1.16E-14 Gy $\cdot$ cm<sup>2</sup> and the corresponding gamma contamination is 1.87E-13 Gy $\cdot$ cm<sup>2</sup>.

Table 3 shows a comparison between our calculated in-air parameters and some of BNCT facilities, which are reactor or proton accelerator based.

### 3.3. Dose calculation

Fig. 11 shows neutron flux profiles for thermal, epithermal and fast neutrons inside the head phantom. This energy spectrum generated from the proposed BSA can reach the maximum in thermal flux at about

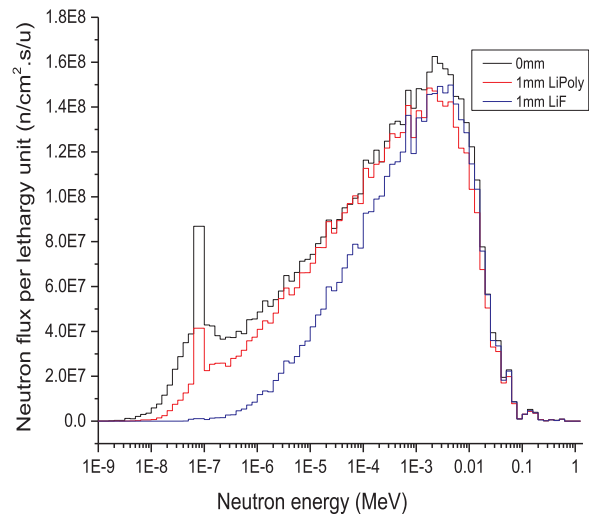


Fig. 8. Flux outside BSA depending filters thicknesses.

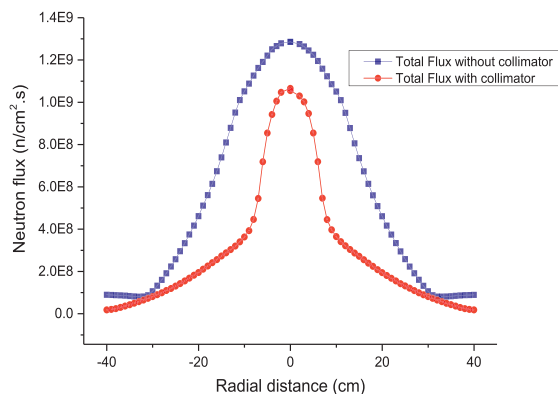
2.78 cm and attenuated at about 12 cm in depth inside the phantom.

Simulated neutron doses in healthy tissue show that the main components are due to boron dose in the brain followed by the gamma dose and fast neutron collision with the hydrogen in the skin (Fig. 12).

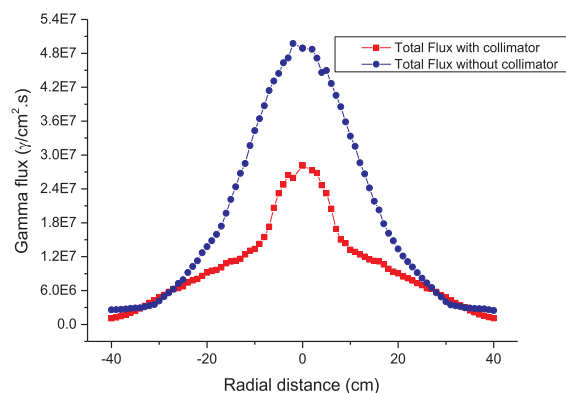
In tumor the advantage depth (AD) defined as the maximum depth at which the tumor dose exceeds the maximum healthy tissue dose is 9.7 cm.

The maximum depth for which the tumor dose is double of the healthy one, the treatable depth (TD), in this case is 7.52 cm.

To define the total doses, which can be delivered by this BSA, we normalize the doses to the maximum punctual healthy tissue dose seated to 11 RBE-Gy, because the other limits of dose prescription (Herrera et al., 2011) are lower to be reached in our case. Where, the maximum punctual skin dose and mean brain dose limited to 16.7 RBE-Gy and 7 RBE-Gy, respectively.



(a) Neutron flux.



(b) Gamma flux.

Fig. 7. : Fluxes at the beam port of the cylindrical collimator and without collimator, as a function of the distance from the axis of the beam.

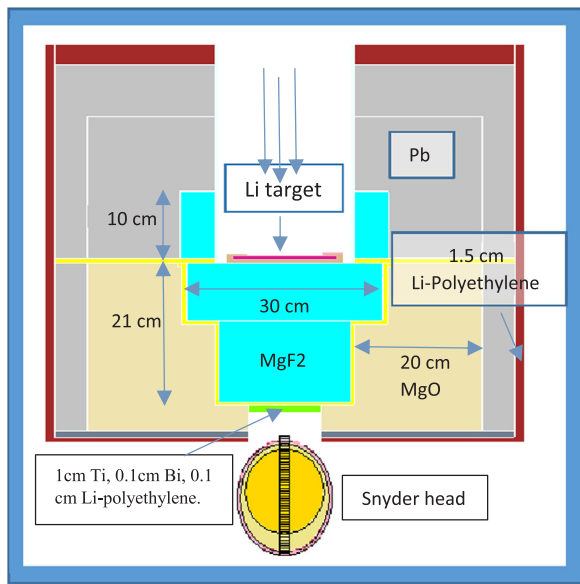


Fig. 9. The final designed BSA.

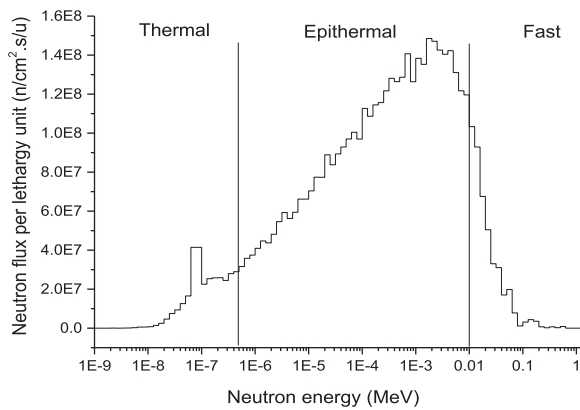


Fig. 10. Neutron spectrum at beam port of the optimized BSA.

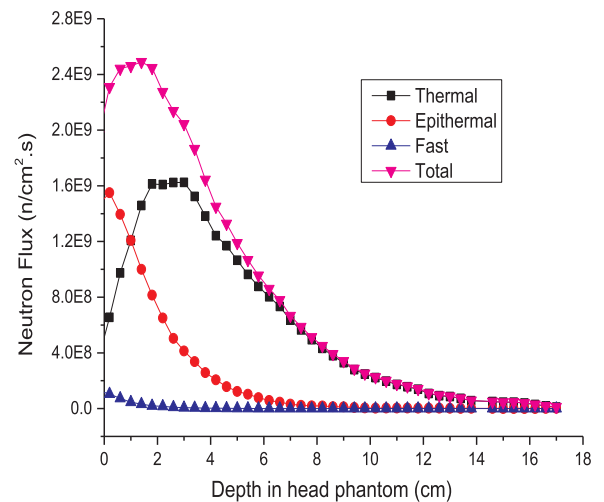


Fig. 11. Neutron flux profiles in head phantom.

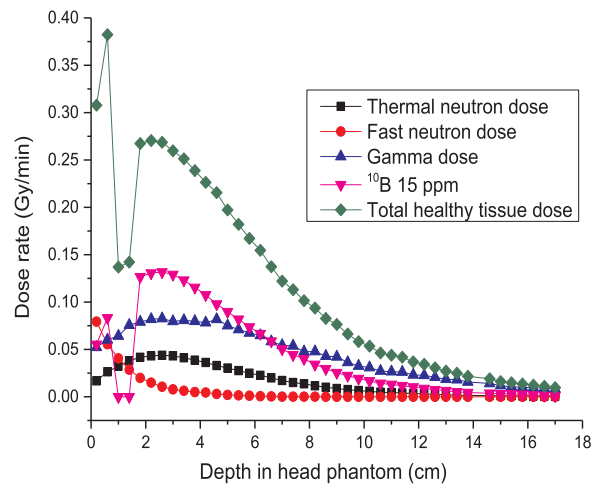


Fig. 12. Dose profiles in healthy tissue.

Table 3  
Beam parameters of our BSA configuration and some published works.

Beam parameters	Neutron yield (x10 <sup>14</sup> n/s)	φ <sub>epi</sub> (x10 <sup>9</sup> n/cm <sup>2</sup> s)	D <sub>fn</sub> /φ <sub>epi</sub> (x10 <sup>-13</sup> Gy.cm <sup>-2</sup> )	D <sub>g</sub> /φ <sub>epi</sub> (x10 <sup>-13</sup> Gy.cm <sup>-2</sup> )	φ <sub>epi</sub> /φ <sub>thermal</sub>	J/φ
IAEA criteria	–	(0.5–1)	< 2	< 2	> 20	> 0.7
Our work	5.78E-2	1.04	1.25	1.89	29.4	0.657
(Cerullo et al., 2002)	4	2.51	3.45	0.21	114.5	0.57
(Rasouli et al., 2012)	1.45	4.43	0.59	1.98	121.2	0.61
(Rahmani and Shahrhiri, 2011)	–	0.819	7.98	1.18	–	–

After renormalizing the doses in order that the maximum healthy punctual tissue dose is 11RBE-Gy, the total tumor and healthy tissue dose profiles have been obtained (Fig. 13). The normalization factor corresponds to the maximum treatment time of 40 min for which a 2.77 RBE-Gy mean dose is delivered to skin with maximum punctual dose of 15.58 RBE-Gy and a mean of 3.71 RBE-Gy to healthy brain tissue. During this time of irradiation the mean tumor dose of 56.5 RBE-Gy with a minimum tumor dose of 52.2 RBE-Gy can be reached, while a therapeutic ratio of tumor to normal tissue is 5.38.

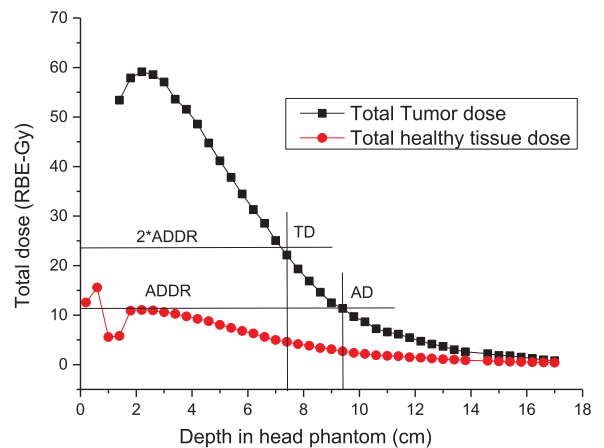


Fig. 13. Dose profiles in tumor and healthy tissue during maximum treatment time.

Table 4 reports in-phantom parameters of different published works.

The Fig. 14 shows longitudinal section in the head-phantom of the deposited energy of neutrons (a) and gamma rays (b), where the red and blue colors are representative for maximum and minimum-deposited energy, respectively.

**Table 4**  
In-phantom parameters of our BSA configuration and some published works.

Facility	ADDR (cGy/min)	AD (cm)	TT (min)	TD (cm)	Tumor: normal tissue 10B concentration (ppm)	Maximum therapeutic ratioTR
Present work, 10 mA 2.3 MeV	126.93	9.7	40	7.52	52.5:15	5.38
(Minsky and Kreiner, 2014) 30 mA, 2.3 MeV	–	–	58.6	5.38	52.5:15	–
(Kononov et al., 2004) 10 mA,	100	9.1	12.5	–	65:18	–
(Rasouli et al., 2012)	41.3	9.4	30.2	7	40:11.42	–
(Rahmani and Shahriari, 2011)	37.1	8.2	34	6.5	65:18	5.05
THOR	50	8.9	25	5.6	65:18	6

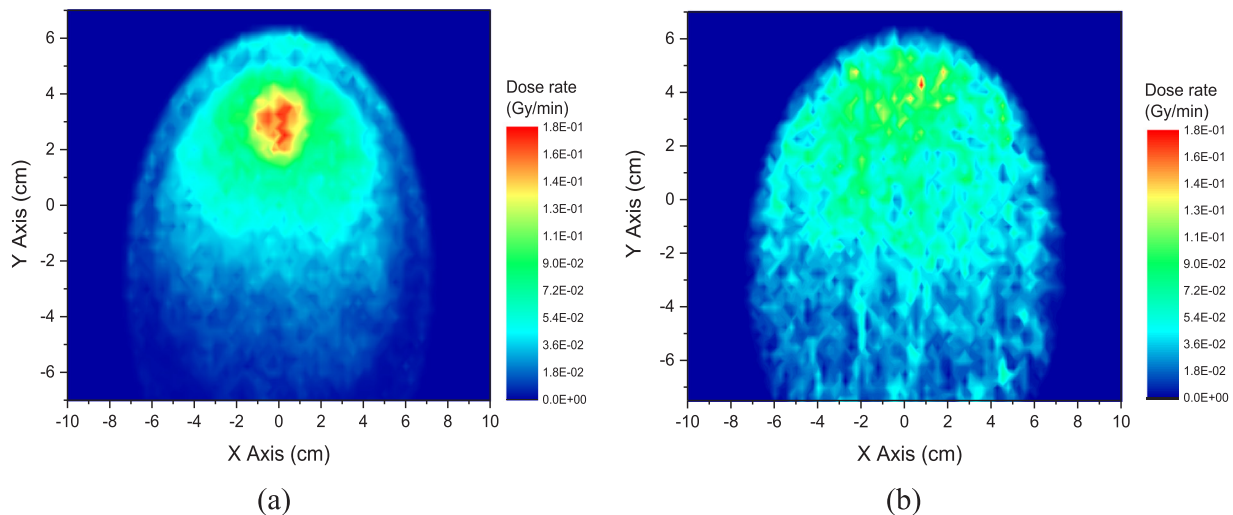


Fig. 14. Deposited energy of neutrons (a) and gamma rays (b) in the head phantom.

#### 4. Conclusion

By means of numerical simulations, the optimization results of the main elements of the beam shaping assembly (neutron source, moderator, shielding, collimator and filters) are reported, suggesting the feasibility of a simple, cheaper and flexible neutron beam facility with low proton energy.

The basic criterion used in designing various components of the BSA was the optimization of the tumor dose delivery to the tumor in short time with consequent background dose reduction.

It was found that to increase therapeutic neutron beam in case of  ${}^7\text{Li}$  (p,n) ${}^7\text{Be}$  reaction neutron source it is suitable to use MgO as a reflector material instead of carbon or lead usually used, with the combination of MgF<sub>2</sub> moderator. This combination leads to generate a biggest amount of useful neutrons with fewer contaminations. For filters, only 1 mm enriched Lithium-Polyethylene and Bi could be efficient.

In addition, an energy proton of 2.3 MeV at 10 mA is enough to generate a satisfactory neutron yield with relatively soft energy.

The results with the shape and materials considered show good treatment possibilities, for which a maximum treatment time is 40 min where a tumor dose can reach 56.5 RBE-Gy. The maximum dose ratio of tumor to normal tissue is 5.38, and the treatable depth is at about 7.52 cm.

#### Acknowledgements

The authors are thankful to the BNCT team in Budker Institute of Nuclear Physics BINP for the research support. The Ministry of Higher Education and Scientific Research of Algeria is gratefully acknowledged for financial support. We thank H. Mazrou for using MCNP code for calculations.

The study was supported by the grant from Russian Science

Foundation (project N° 14-32-00006), Budker Institute of Nuclear Physics and Novosibirsk State University.

#### References

- Bayanov, B., Belov, V., Kindyuk, V., Oparin, E., Taskaev, S., 2004. Lithium neutron producing target for BINP accelerator-based neutron source. *Appl. Radiat. Isot.* 61, 817–821. <http://dx.doi.org/10.1016/j.apradiso.2004.05.032>.
- Bayanov, B.F., 1998. Accelerator based neutron source for the neutron-capture and fast neutron therapy at hospital. *Nucl. Instrum. Methods Phys. Res. A* 413, 397–426. [http://dx.doi.org/10.1016/S0168-9002\(98\)00425-2](http://dx.doi.org/10.1016/S0168-9002(98)00425-2).
- Busse, P., Harling, O.K., Palmer, M.R., Iii, W.S.K., Kaplan, J., I, I.K., Chuang, C.E., Goorley, J.T., Riley, K.J., Newton, T.H., Cruz, G.A.S., I, X.L., Zamenhof, R.G., 2003. A critical examination of the results from the Harvard-mit NCT program phase I clinical trial of neutron capture therapy for intracranial disease. *J. Neurooncol.* 62, 111–121.
- Ceballos, C., Esposito, J., Agosteo, S., Colautti, P., Conte, V., Moro, D., Pola, A., 2011. Towards the final BSA modeling for the accelerator-driven BNCT facility at INFN LNL. *Appl. Radiat. Isot.* 69, 1660–1663. <http://dx.doi.org/10.1016/j.apradiso.2011.01.032>.
- Cerullo, N., Esposito, J., Leung, K.N., Custodero, S., 2002. *Rev. Sci. Instrum.* 73, 3614–3618.
- Culbertson, C.N., Green, S., Mason, A.J., Picton, D., Baugh, G., Hugtenburg, R.P., Yin, Z., Scott, M.C., Nelson, J.M., 2004. In-phantom characterisation studies at the Birmingham Accelerator-Generated epithermal Neutron Source. *Appl. Radiat. Isot.* 61, 733–738. <http://dx.doi.org/10.1016/j.apradiso.2004.05.057>.
- Drog, M., 2005. DROSG-2000:Neutron Source Reactions. IAEA-NDS-87 Rev. 9.
- Esposito, J., Colautti, P., Fabritsiev, S., Gervash, A., Giniyatulin, R., Lomasov, V.N., Makhankov, A., Mazul, I., Pisent, A., Rumyantsev, M., Tanchuk, V., Tecchio, L., 2009. Be target development for the accelerator-based SPES-BNCT facility at INFN Legnaro. *Appl. Radiat. Isot.* 67 (7–8, Supple. 1), S270–S273.
- Eskandari, M.R., Kashian, S., 2009. Design of moderator and multiplier systems for D-T neutron source in BNCT. *Ann. Nucl. Energy* 36, 1100–1102. <http://dx.doi.org/10.1016/j.anucene.2009.05.005>.
- Goorley, J.T., Kiger, W.S., Zamenhof, R.G., 2002. Reference dosimetry calculations for neutron capture therapy with comparison of analytical and voxel models. *Med. Phys.* 29, 145–156. <http://dx.doi.org/10.1118/1.1428758>.
- Herrera, M.S., González, S.J., Minsky, D.M., Kreiner, A.J., 2013. Evaluation of performance of an accelerator-based BNCT facility for the treatment of different tumor targets. *Phys. Medica* 29, 436–446. <http://dx.doi.org/10.1016/j.ejmp.2013.01.006>.
- IAEA, 2001. Current status of neutron capture therapy. IAEA-TECDOC-1223.
- Kasatov, D., Makarov, A., Shchudlo, I., Taskaev, S., 2015. A study of gamma-ray and

- neutron radiation in the interaction of a 2MeV proton beam with various materials. *Appl. Radiat. Isot.* 106, 38–40. <http://dx.doi.org/10.1016/j.apradiso.2015.08.011>.
- Kiger, S., Sakamoto, S., Harling, O., 1999. Neutronic design of a fission converter-based epithermal neutron beam for neutron capture therapy neutron beam for neutron capture therapy. *Nucl. Sci. Eng.* 131, 1–22. <http://dx.doi.org/10.13182/NSE99-A2015>.
- Kononov, O.E., Kononov, V.N., Bokhovko, M.V., Korobeynikov, V.V., Soloviev, A.N., Sysoev, A.S., Gulidov, I.A., Chu, W.T., Nigg, D.W., 2004. Optimization of an accelerator-based epithermal neutron source for neutron capture therapy. *Appl. Radiat. Isot.* 61, 1009–1013. <http://dx.doi.org/10.1016/j.apradiso.2004.05.028>.
- Lee, C.L., Zhou, X., 1999. Thick target neutron yields for the  ${}^7\text{Li}(p,n){}^7\text{Be}$  reaction near threshold. *Nucl. Inst. Methods Phys. Res. B* 152, 1–11.
- Lee, C.L., Zhou, X.L., Kudchadker, R.J., Harmon, F., Harker, Y.D., 2000. A Monte Carlo dosimetry-based evaluation of the  ${}^7\text{Li}(p,n){}^7\text{Be}$  reaction near threshold for accelerator boron neutron capture therapy. *Med. Phys.* 27, 192–202. <http://dx.doi.org/10.1118/1.598884>.
- Minsky, D.M., Kreiner, A.J., 2014. Beam shaping assembly optimization for  ${}^7\text{Li}(p,n){}^7\text{Be}$  accelerator based BNCT. *Appl. Radiat. Isot.* 88, 233–237. <http://dx.doi.org/10.1016/j.apradiso.2013.11.088>.
- Monshizadeh, M., Kasesaz, Y., Khala, H., Hamidi, S., 2015. Progress in Nuclear Energy MCNP design of thermal and epithermal neutron beam for BNCT at the Isfahan MNSR. *Prog. Nucl. Energy J.* 83, 427–432. <http://dx.doi.org/10.1016/j.pnucene.2015.05.004>.
- Palmer, M.R., Goorley, J.T., Kiger III, W.S., Busse, P.M., Riley, K.J., Harling, O.K., Zamenhof, R.G., 2002. *Int. J. Radiat. Oncol. Biol. Phys.* 53, 1361–1379.
- Rahmani, F., Shahriari, M., 2011. Beam shaping assembly optimization of Linac based BNCT and in-phantom depth dose distribution analysis of brain tumors for verification of a beam model. *Ann. Nucl. Energy* 38, 404–409. <http://dx.doi.org/10.1016/j.anucene.2010.10.001>.
- Rasouli, F.S., Masoudi, S.F., Kasesaz, Y., 2012. Annals of Nuclear Energy Design of a model for BSA to meet free beam parameters for BNCT based on multiplier system for D – T neutron source. *Ann. Nucl. Energy* 39, 18–25. <http://dx.doi.org/10.1016/j.anucene.2011.08.025>.
- Saurwein, W.A.G., Wittig, A., Moss, R., Nakagawa, Y., 2012. Neutron Capture Therapy: Principles and Applications. Springer <http://dx.doi.org/10.1007/978-3-642-31334-9>.
- Sakamoto Iii, S., W.S.K., Harling, O.K., 1999. Sensitivity studies of beam directionality , beam size , and neutron spectrum for a fission converter-based epithermal neutron beam for boron neutron capture therapy. *Med. Phys.* 26, 1979–1988.
- Taskaev, S., 2015. Accelerator based epithermal neutron source. *Phys. Part. Nucl.* 46, 956–990. <http://dx.doi.org/10.1134/S1063779615060064>.
- X-5 Monte Carlo Team, 2003. MCNP — A General Monte Carlo N-Particle Transport Code, Version 5, LA-UR-03-1987.
- Zaidi, L., Kashaeva, E., Lezhnin, S., Malyshkin, G., Samarin, S., T, S., Taskaev, S., Frolov, S., 2017. Neutron-beam-shaping assembly for boron neutron-capture therapy. *Phys. At. Nucl.* 80, 60–66. <http://dx.doi.org/10.1134/S106377881701015X>.
- Zhou, X.-L., Lee, C., 1997. Lithium compounds as targets for (p,n) reactions. *Appl. Radiat. Isot.* 48, 1493–1496. [http://dx.doi.org/10.1016/S0969-8043\(97\)00145-0](http://dx.doi.org/10.1016/S0969-8043(97)00145-0).